Microseismic event azimuth estimation: establishing a relationship between hodogram linearity and uncertainty in event azimuth

Julian Drew and Robert White , University of Cambridge, James Wolfe, BP North America Gas*

Summary:

For microseismic data monitored and detected by a downhole vertical array, the polarization, or hodogram information, is needed to determine the event azimuth. To optimally weight when averaging over multiple measurements, we require knowledge of the uncertainties associated with each estimate.

We discuss data acquired during a hydraulic stimulation. Using both synthetic data and observed events, by experiment we establish a relationship between the uncertainty in the estimated azimuth (or error), the signal-to-noise ratio, and hodogram rectilinearity.

Introduction:

In 2006, a hydraulic fracture stimulation was made in a horizontal well, of the Mesozoic section of clastic tight gas reservoir in the Rocky Mountains of North America. Seismicity was monitored both before and during injection, by a vertical seismic array deployed in an offset monitoring well.

Over 1000 induced microseismic events were detected by the array during four hours of injection. The distance and vertical location of an event relative to the array can be determined by measuring and inverting phase arrival times. The azimuth of an event with respect to the array can be determined by analyzing the polarization of the phase arrivals.

While there is a good understanding of errors associated with arrival times, there is no well established relationship between the measured arrival polarization, and the uncertainty of the estimate of the azimuth.

We discuss two measures of hodgram quality, the signal-to-noise ratio and the hodogram rectilinearity. All data is analyzed over a 90-200 Hz bandwidth.

Geometry

A plan and elevation view for the survey is shown in Figure 1. The seismic array was offset some 400m from a horizontal injection well. The array comprised 32 levels of three-component DDS-250 Oyo Geospace seismic shuttles, each shuttle having a 15Hz omni-2400 dual element geophone.

Level 12 to Level 31 were deployed as ten shuttle pairs, each pair being rigidly attached together, and thus at a fixed orientation. This gives 22 separate levels in depth, each separated by a 15m flexible bridle, for a total array length of 320m.

An explosive charge (shot) was detonated in the vertical section of the injection well to allow the orientation of the tools to be estimated. Arrivals were picked, hodograms analyzed, and an estimate of orientation of the tool (sensor) made for each separate level.

In our analysis of measured hodograms we make use of the shuttle pairs. Since each pair is at a fixed orientation, our results are independent of knowing the precise orientation of the tools.

We have chosen to limit the analysis to a selection of four pairs (eight levels). Levels 22/23 and 28/29 exhibited the most consistent hodograms and azimuth estimates for the array. Levels 12/13 and 16/17 were characteristic of the excluded data. Of the excluded data, one signal showed a degree of phase distortion, possibly from a malfunctioning geophone.

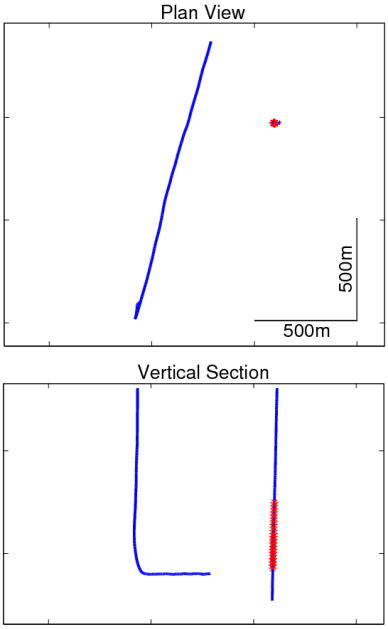

Figure 1: Plan view and vertical section (1:1) of horizontal injection well and vertical monitoring well with 32 level seismic array (red).

Synthetic Signal

In order to test for a relationship, we added a synthetic signal to the measured noise for each of the levels. The synthetics were for multiple azimuths and at incremental signal-to-noise levels. The results showed little variation with choice of azimuth, so all azimuths have been included. In total, more than 50,000 hodograms were analyzed at each noise level.

The distribution of errors in the estimated azimuth at four different noise levels is plotted in Figure 2. When the standard deviation in azimuth error is plotted against signal-to-noise ratio, as in Figure 3, we find that a log-log relationship holds. The relationship appears to change for choice of seismic level; the curves do not over-plot (Figure 3). It is likely that each tool has its own noise characteristic.

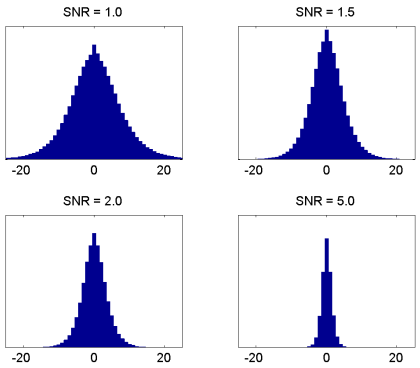

Figure 2: Distribution of error in azimuth, at four signal-to-noise (snr) levels. Result computed by adding a synthetic signal to the recorded noise.

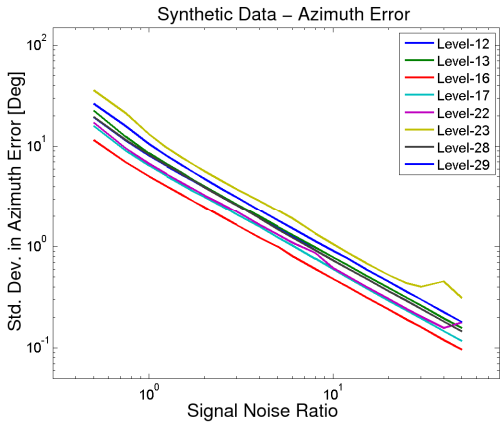

Figure 3: Log-log relationship observed between signal to noise ratio, and the standard deviation in azimuth (error), for a synthetic signal added to measured noise.

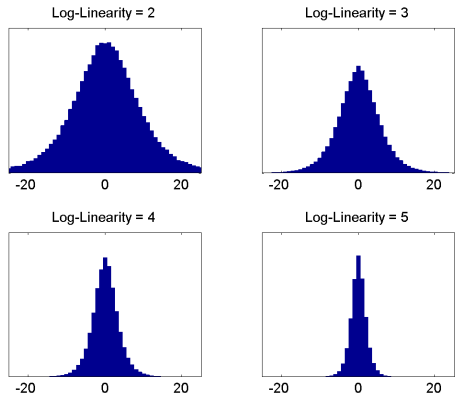

Figure 4: Distribution of error in azimuth, at four hodogram log-linearity values. Synthetic signal added to recorded noise.

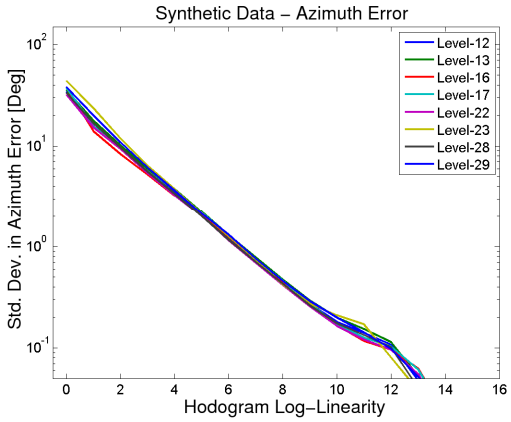

Figure 5: Standard deviation of error in azimuth plotted against the log of the hodogram linearity. Synthetic signal added to measured noise.

In computing the hodogram we obtain a hodogram linearity measure, being the ratio of eigenvalues, or equivalently, the ratio of the minor to major axis of the hodogram ellipsoid.

For the hodograms of the synthetics, we have binned (grouped) the results (Figure 4), based on the logarithm of the ratio of the second to first eigenvalue, which we call hodogram log-linearity :

$$LogLinearity = \log {}^{\gamma_1}/_{\gamma_2}$$

Calculating and plotting the standard deviation of error in estimated azimuth against the hodogram log-linearity, (Figure 5), we find that a similar log-linear relationship holds. The curves for each of the seismic levels appear to over-plot better.

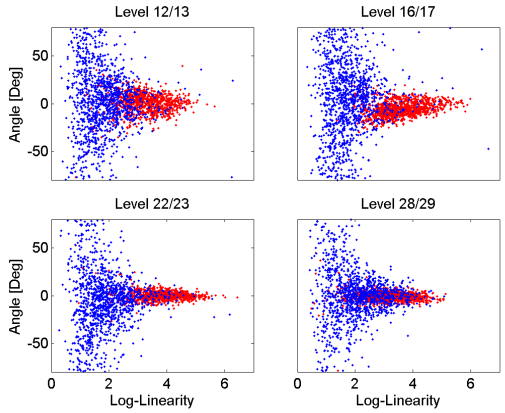

Figure 6: Compressional (P), blue, and Shear (Sh), red. Difference in arrival azimuth, for each of four pairs of seismic level. Results plotted against average of hodogram log-linearity for the arrival.

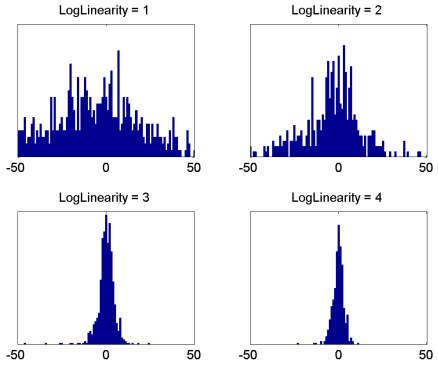

Figure 7: Distribution of angle differences for level 22/23, for four hodogram log-linearity bins.

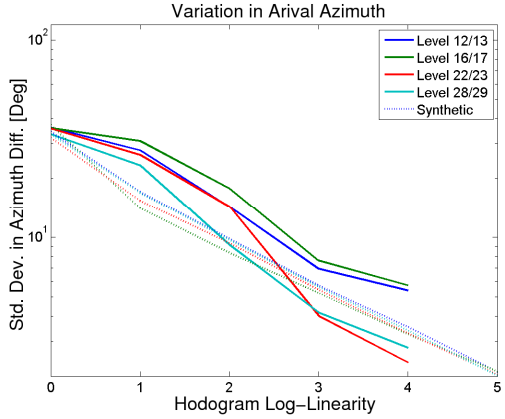

Figure 8: Calculated dependence of azimuth error to hodogram log-linearity. Also plotted are four of the curves generated for synthetic arrivals (dotted lines).

Measured Microseismic Arrivals

A parameter based algorithm (Drew, 2005) was used to identify and locate approximately 1000 events in the dataset, using compressional (P) and shear (Sh) arrivals. The shear arrivals have a higher signal-to-noise ratio than the compressional arrivals. It is useful therefore to use the shear hodogram to pick the source azimuth (Eisner, 2008, Geoph. J. Int., submitted).

To improve the statistics of the data and have a wide range of signal-to-noise levels we have created a single dataset by combining the shear and compressional data for each of the four pairs of levels (Figure 6). We have binned the data by hodogram log-linearity into unit bins from 0-4. The distribution of angle differences (errors) for one pair is show in Figure 7.

We have computed the standard deviation of angle difference for each pair, and plotted the results in Figure 8. The value has been scaled by 1/sqrt(2), as the angle "error" estimate is a difference of two angles and hence the sum of two errors.

The synthetic results have been over-plotted (dotted lines) in Figure 8. Although the statistics are poor, the results are surprisingly consistent. The data suggests that the linearity of hodogram is a good measure of the quality of the azimuth estimate.

Computing the covariance matrix in the frequency domain, an azimuth and linearity value can be computed at each frequency (Moriya, 1994). In Figure 9, we plot the results for selected frequencies between 90 to 200 Hz. The results are consistent with those obtained for the time domain covariance matrix (Figure 8).

Fitting a line to the synthetic observations, we obtain the following relationship:

$$\log \sigma_\theta = -0.512 \log {}^{\gamma_1}/_{\gamma_2} + 3.33$$

As the distribution of angles is bounded (circular) it would be appropriate to fit a von Mises distribution (Fisher, 1993).

Application

In addition to establishing suitable weights when averaging over multiple measurements, in Figure 10 we show the application to a method of interactive analysis. The lower panel shows the chosen window of the time domain signal, for a shear Sh arrival. The center panel shows the hodogram azimuth and inclination; the upper panel the results from the spectral matrix analysis.

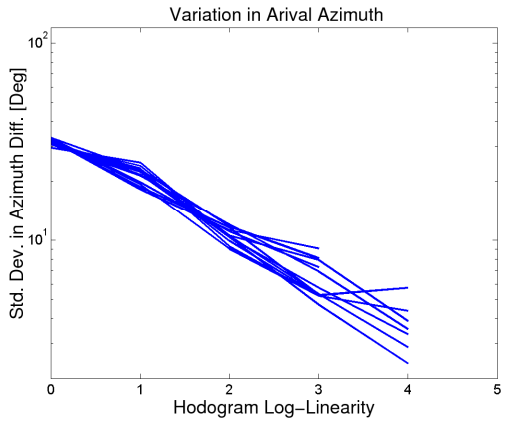

Figure 9: Dependence of azimuth error on hodogram log-linearity, for level 22/23, computed by the spectral matrix method. Curves are plotted for frequencies 90-200 Hz.

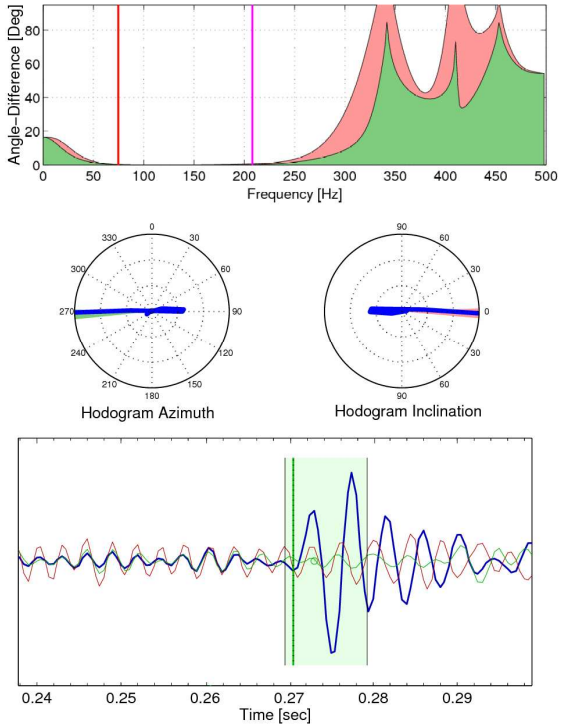

Figure 10: Spectral analysis of a hodogram. The upper panel shows the variation of azimuth of the hodogram by the spectral matrix method, including an error estimate calculated from the hodogram log-linearity. The center panel plots the hodogram of the signal.

The green curve of the upper panel highlights the deviation in azimuth of the spectral hodogram. A value of zero is the spectral hodogram consistent with the picked arrival direction. Plotting the result as the angle between two vectors, being the picked hodogram and the hodogram at each frequency, gives us the comparative result as a 2D plot. The orange/pink curve adds an additional angle uncertainty, calculated from the spectral hodogram log-linearity, using the relationship given above.

The chosen bandwidth for analysis of the hodogram is shown as the vertical lines on the upper panel, Figure 10. Careful analysis and choice of bandwidth is important. Resonances resulting from tool design and coupling performance; sensor and instrument response (such as sensor spurious frequency) impact spectrally on the hodogram result.

Using this method of analysis we identified the bandwidth of 90-200Hz as the most suitable. Above 200Hz, tool coupling and tool resonance affect the hodogram; below 90Hz, the data is more noisy.

Conclusions

We have shown for synthetic signals and measured arrivals that a linear relationship holds between the log of the hodogram linearity, and the log of the uncertainty in measured hodogram angle.

This relationship can be used to quantify uncertainty in estimated arrival angles. When averaging over multiple measurements to estimate event location, the quantified uncertainty provides a basis for calculating suitable weights.

Acknowledgments

The authors wish to thank BP North America Gas for permission to use the data and publish the results, and Brian Hornby and Frederik Tilmann for their comments.

EDITED REFERENCES

Note: This reference list is a copy-edited version of the reference list submitted by the author. Reference lists for the 2008 SEG Technical Program Expanded Abstracts have been copy edited so that references provided with the online metadata for each paper will achieve a high degree of linking to cited sources that appear on the Web.

REFERENCES

Drew, J., D. Leslie, P. Armstrong, and G. Michaud, 2005, Automated microseismic event detection and location by continuous spatial mapping: Paper SPE 95513, SPE.

Fisher, N., 1993, Statistical analysis of circular data: Cambridge.

Moriya, H., K. Nagano, and H. Niitsuma, 1994, Precise source location of AE doublets by spectral matrix analysis of triaxial hodogram: Geophysics, **59**, 36–45.